

Spatial-Temporal BEM and Channel Estimation Strategy for Massive MIMO Time-Varying Systems

Hongxiang Xie*, Feifei Gao*, Shun Zhang[†], and Shi Jin[‡]

* Tsinghua National Laboratory for Information Science and Technology (TNList), Beijing

[†] State Key Laboratory of Integrated Services Networks, Xidian University

[‡] National Communications Research Laboratory, Southeast University

Abstract—This paper proposes a new channel estimation scheme for the multiuser massive multiple-input multiple-output (MIMO) systems in time-varying environment. We introduce a discrete Fourier transform (DFT) aided spatial-temporal basis expansion model (ST-BEM) to reduce the effective dimensions of uplink/downlink channels, such that training overhead and feedback cost could be greatly decreased. The newly proposed ST-BEM is suitable for both time division duplex (TDD) systems and frequency division duplex (FDD) systems thanks to the angle reciprocity, and can be efficiently deployed by fast Fourier transform (FFT). Various numerical results have corroborated the proposed studies.

Index Terms—Massive MIMO, spatial-temporal BEM, DFT, DOA, angle reciprocity.

I. INTRODUCTION

Channel estimation has been a major challenge for massive multiple-input multiple-output (MIMO) system, where most existing works, e.g. [1], focus on time-invariant environments. However, in many mobile environment, the time varying channel estimation should also be considered so as to improve the accuracy of data detection.

Since channel parameters cannot change in a sudden way in time domain, one may expect correlation among the time varying channel parameters. Exploiting this fact, the conventional studies try to reduce the number of the channel parameters by the following three approaches: (1) Gauss-Markov model [2], which captures channel variation through symbol-by-symbol updating; (2) basis expansion model (BEM) [3], which decomposes channels into the superposition of time-varying basis functions weighted by time-invariant coefficients; (3) known temporal channel covariance matrix, whose most dominant eigenvectors can act as basis vectors to span the time varying channels. Among these approaches, BEM approach has attracted most attentions due to its easier implementation, while channel covariance matrix approach suffers from huge complexity and overhead cost.

Similarly, for massive MIMO system with closely equipped array antennas, the channels are also highly correlated in the spatial domain. Based on this fact, [4] and [5] assume the spatial channel covariance matrix is known and use the dominant eigenvectors to span the spatial channels. A natural

This work was supported in part by the National Natural Science Foundation of China under Grant {61422109, 61531011}.

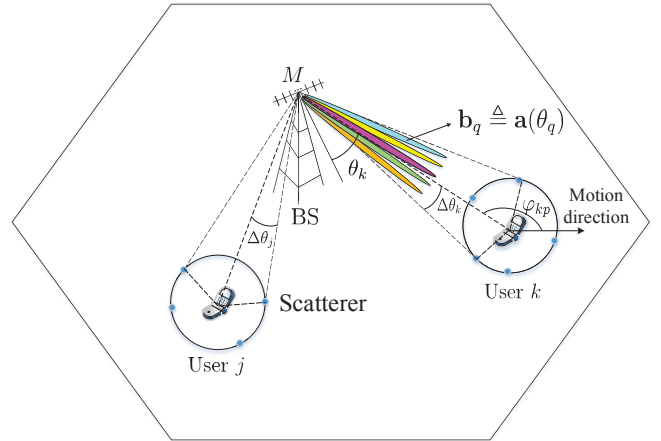


Fig. 1. System model. Users are surrounded by P local scatterers and the mean DOA and AS of user- k are θ_k and $\Delta\theta_k$, respectively. When users move around in the circle, the spatial AS seen by BS is generally unchanged.

question then arises: does there exist a simpler counterpart of temporal BEM to reduce the spatial channel dimension?

Motivated by this, we propose a discrete Fourier transform (DFT) based spatial basis expansion model (SBEM) for massive uniform linear array (ULA). Meanwhile, we also jointly consider the temporal basis expansion model under time selective environment, resulting into the spatial-temporal BEM (ST-BEM) that could efficiently reduce the channel parameters both in time and spatial domains. Importantly, the proposed framework is suitable for both TDD and FDD systems by exploiting the angle reciprocity, and can be efficiently implemented by the fast Fourier transform (FFT) and partial FFT. Various numerical results are provided to corroborate the proposed scheme.

II. SYSTEM MODEL AND CHANNEL CHARACTERISTICS

A. System Model

Let us consider a multiuser massive MIMO system, where BS is equipped with $M \gg 1$ antennas in the form of ULA serving K single-antenna users and each user is surrounded by a circle of P local scatterers, as shown in Fig. 1. Considering the motion of users, the baseband channels between users and BS are assumed to be time-selective flat-fading. Note that as users move around within the circular area, the spatial directions of users seen by the BS can be viewed as unchanged,

until users' locations have significantly changed. Hence, the propagation from user- k to BS is assumed to consist of $P \gg 1$ rays and the corresponding $M \times 1$ uplink channel at time index n can be expressed as [5], [6]:

$$\mathbf{h}_k(n) = \frac{1}{\sqrt{P}} \sum_{p=1}^P \alpha_{kp} e^{-j(2\pi f_d n T_s \cos \varphi_{kp} + \phi_{kp})} \mathbf{a}(\theta_{kp}), \quad (1)$$

for $n = 0, \dots, N-1$, where α_{kp} denotes the time-varying complex gain of the p -th ray; f_d is the maximum Doppler frequency; T_s is the system sampling period; φ_{kp} is the angle between the user- k 's uplink transmitted signal and its motion direction (see Fig. 1); ϕ_{kp} signifies the initial phase, which is uniformly distributed in $[0, 2\pi]$; α_{kp} 's, φ_{kp} 's and ϕ_{kp} 's are independent and identical distributed (i.i.d.) among different rays. Moreover, $\mathbf{a}(\theta_{kp}) \in \mathbb{C}^{M \times 1}$ is the array manifold vector defined as

$$\mathbf{a}(\theta_{kp}) = \left[1, e^{j\frac{2\pi d}{\lambda} \sin \theta_{kp}}, \dots, e^{j\frac{2\pi d}{\lambda} (M-1) \sin \theta_{kp}} \right]^T, \quad (2)$$

where d is the antenna spacing, λ is the signal wavelength, and θ_{kp} is the direction of arrival (DOA) of the p -th ray seen by the BS array.

Similar to [4] and [5], the incident angular spread (AS) of user- k with mean DOA θ_k seen by BS is assumed to be limited in a narrow region, i.e., $[\theta_k - \Delta\theta_k, \theta_k + \Delta\theta_k]$. And this spatial AS of each user is generally unaltered when the user moves within the circular area, see Fig. 1. Hence, there exists high correlations among $\mathbf{a}(\theta_{kp})$, $p = 1, \dots, P$, and $\mathbf{h}_k(n)$ can be expanded from some orthogonal basis as

$$\mathbf{h}_k(n) = \sum_{q=1}^{\tau} \psi_{k,q}(n) \mathbf{b}_q, \quad 0 \leq n \leq N-1. \quad (3)$$

As long as we find a set of uniform basis vectors \mathbf{b}_q 's (i.e., the colored beams in Fig. 1) for any possible $\mathbf{h}_k(n)$ and for any time $0 \leq n \leq N-1$, then the task of channel estimation will be greatly simplified to estimating τ ($\ll M$) expansion coefficients $\psi_{k,q}(n)$'s only.

To capture the rapid variation of $\psi_{k,q}(n)$'s, the complex componential basis expansion model (CE-BEM) [3] is applied in this paper so that during any time interval of NT_s , $\psi_{k,q}(n)$'s can be modeled as [7], [8]

$$\psi_{k,q}(n) = \sum_{r=0}^R \lambda_{k,q}^r e^{j2\pi(r-R/2)n/N}, \quad 0 \leq n \leq N-1, \quad (4)$$

where $\lambda_{k,q}^r$'s are the CE-BEM coefficients that remain invariant within one interval of NT_s but may vary in the next interval. Note that the order of the bases R is a function of the channel bandwidth and the interval length.

B. Characteristics of Channels in Space and Time Domain

Define the normalized DFT of the channel vector $\mathbf{h}_k(n)$ as $\tilde{\mathbf{h}}_k(n) = \mathbf{F} \mathbf{h}_k(n)$, where \mathbf{F} is the $M \times M$ DFT matrix whose (p, q) th element is $[\mathbf{F}]_{pq} = e^{-j\frac{2\pi}{M} pq} / \sqrt{M}$.

Property 1: For the channel model (1), $\tilde{\mathbf{h}}_k(n)$ is approximately a sparse vector with most channel power concentrated on few DFT entries.

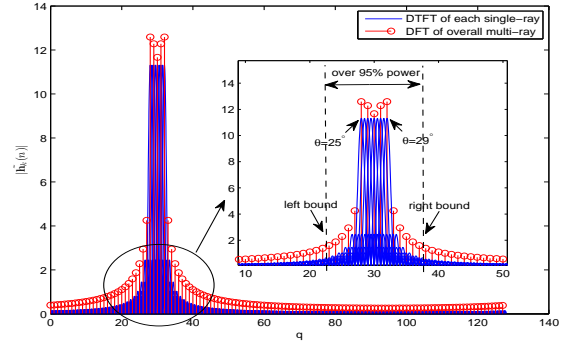


Fig. 2. Example of the DFT of channel model $\mathbf{h}_k(n)$ with DOA inside $[25^\circ, 29^\circ]$ and $M = 128, d = \lambda/2$. Since the AS is unchanged for the whole interval, the position of \mathcal{B}_k is also the same for all $0 \leq n \leq N-1$.

Proof: Based on the Vandermonde structure of $\mathbf{a}(\theta_{kp})$, the property is comprehensible. To illustrate this, let us define \mathcal{B}_k as the index set of the continuous DFT points that contain at least η portion of the total channel power. Then the left bound of \mathcal{B}_k is determined by the DFT of the leftmost ray with $\theta_{kp} = \theta_k - \Delta\theta_k$ and can be expressed as $\lceil M \frac{d}{\lambda} \sin(\theta_k - \Delta\theta_k) \rceil - \lceil B_{\max}/2 \rceil$, where B_{\max} is the upper bound of the cardinality of \mathcal{B}_k , i.e., $|\mathcal{B}_k|$, corresponding to any single-ray case with DOA inside $[\theta_k - \Delta\theta_k, \theta_k + \Delta\theta_k]$, and $\lceil \cdot \rceil$ and $\lfloor \cdot \rfloor$ denote the integer ceiling and integer floor, respectively. Similarly, the right bound of \mathcal{B}_k depends on the DFT of the rightmost ray with $\theta_{kp} = \theta_k + \Delta\theta_k$ and can be expressed as $\lceil M \frac{d}{\lambda} \sin(\theta_k + \Delta\theta_k) \rceil + \lceil B_{\max}/2 \rceil$. Then for any single ray with incident DOA inside $[\theta_k - \Delta\theta_k, \theta_k + \Delta\theta_k]$, $|\mathcal{B}_k|$ can be approximated as

$$\begin{aligned} |\mathcal{B}_k| &\approx \lceil M \frac{d}{\lambda} \sin(\theta_k + \Delta\theta_k) \rceil - \lfloor M \frac{d}{\lambda} \sin(\theta_k - \Delta\theta_k) \rfloor + 1 + B_{\max} \\ &\approx \lceil 2M \frac{d}{\lambda} \cdot |\cos \theta_k| \cdot \Delta\theta_k + 1 \rceil + B_{\max}. \end{aligned} \quad (5)$$

To demonstrate this, an example of a 9-ray channel with AS $[25^\circ, 29^\circ]$ is given in Fig. 2, where the discrete time Fourier transform (DTFT) of each single ray as well as the DFT of overall multi-rays are depicted respectively. This numerical simulation shows that the actual cardinality of \mathcal{B}_k containing $\eta = 95\%$ power is 15, which is just equal to the result of (5).

Based on (5) and recalling that $\Delta\theta_k$ is small, it is obvious that $|\mathcal{B}_k| \approx \lceil \frac{2Md}{\lambda} \cdot |\cos \theta_k| \cdot \Delta\theta_k + 1 \rceil + B_{\max}$ is still small compared to M . Hence, $\tilde{\mathbf{h}}_k(n)$ is approximately sparse with most power being contained in limited number of entries. ■

As per *Property 1*, the key idea of this paper is to approximate the channel vector with fewer parameters as

$$\mathbf{h}_k(n) = \mathbf{F}^H \tilde{\mathbf{h}}_k(n) \approx [\mathbf{F}^H]_{:, \mathcal{B}_k} [\tilde{\mathbf{h}}_k(n)]_{\mathcal{B}_k, :} = \sum_{q \in \mathcal{B}_k} \tilde{h}_{k,q}(n) \mathbf{f}_q, \quad (6)$$

where $\tilde{h}_{k,q}(n) \triangleq [\tilde{\mathbf{h}}_k(n)]_q$ denotes the q -th element of $\tilde{\mathbf{h}}_k(n)$ while \mathbf{f}_q is the q -th column of \mathbf{F}^H ; $[\cdot]_{:, \mathcal{B}_k}$ and $[\cdot]_{\mathcal{B}_k, :}$ denote the sub-matrices by collecting columns or rows indexed by \mathcal{B}_k , respectively. Compare with (3), the expansion in (6) is in the form of BEM where the basis vectors, $\mathbf{b}_q \triangleq \mathbf{f}_q$, are

orthogonal to each other. Hence, we only need to estimate the limited BEM coefficients $\tilde{h}_{k,q}(n)$.

Interestingly, the DFT vector \mathbf{f}_q coincides with the steering vector as $\mathbf{f}_q = \mathbf{a}(\theta_q)$ where $\theta_q = \arcsin \frac{q\lambda}{Md}$, which means that \mathbf{f}_q formulates an array beam towards the physical direction $\theta_q = \arcsin \frac{q\lambda}{Md}$ (see Fig. 1). Hence, all beams \mathbf{f}_q 's inside \mathcal{B}_k will point towards the AS of user- k and are orthogonal to each other. Consequently, the beam indices, i.e., \mathcal{B}_k , are defined as the *spatial signature* of user- k , and (6) can be deemed as the *spatial BEM* (SBEM).

Note that, since the spatial AS for users are unchanged for $0 \leq n \leq N-1$, their spatial signature \mathcal{B}_k will also be the same for the whole interval. This is illustrated in Fig. 2, where the position of \mathcal{B}_k of $\tilde{\mathbf{h}}_k(n)$ is almost the same for all time index $0 \leq n \leq N-1$.

Property 2: All the components of $\tilde{\mathbf{h}}_k(n)$, say $\tilde{h}_{k,q}(n)$, $q = 0, \dots, M-1$, are band-limited and the maximum bandwidth of the power spectra is exactly equal to f_d .

Proof: First let us define the time-domain discrete correlation matrix of $\mathbf{h}_k(n)$ as $\mathbf{R}_k(m) \triangleq \mathbb{E}\{\mathbf{h}_k(n)\mathbf{h}_k^H(n+m)\}$ and then the (i, l) th components of $\mathbf{R}_k(m)$ is given as

$$\begin{aligned} [\mathbf{R}_k(m)]_{i,l} &= \mathbb{E}\{h_{k,i}(n)h_{k,l}^*(n+m)\} \\ &= \frac{1}{P} \sum_{p=1}^P \mathbb{E}\{|\alpha_{kp}|^2\} \mathbb{E}\{e^{-j2\pi f_d m T_s \cos \varphi_{k,p}}\} \\ &\quad \cdot \mathbb{E}\{e^{j\frac{2\pi d}{\lambda}(i-l) \sin \theta_{k,p}}\}, \end{aligned} \quad (7)$$

where $\mathbb{E}\{\cdot\}$ denotes expectation.

It is worth noticing that different from the conventional Clarke's reference model [6], where the incident angles of users' signals seen at the BS are assumed to be uniformly distributed on $[0, 2\pi]$, the spatial AS of user- k here is unchanged within a narrow range, i.e., $[\theta_k - \Delta\theta_k, \theta_k + \Delta\theta_k]$ as discussed before, while the angle φ_{kp} at the user end is assumed to be randomly distributed over $[0, 2\pi]$ for the rich local scatters surrounding the users and the high random mobility of users. Therefore, the expectation in (7) is mainly focused on φ_{kp} and then we have

$$[\mathbf{R}_k(m)]_{i,l} = J_0(2\pi f_d m T_s) \cdot g(2\pi d/\lambda(l-i)), \quad (8)$$

where $J_0(x) = \frac{1}{2\pi} \int_{-\pi}^{\pi} e^{-jx \cos y} dy$ is the zero-order Bessel function of the first kind, and $g(\cdot)$ is similarly defined as $g(x) = \frac{1}{2\Delta\theta_k} \int_{\theta_k - \Delta\theta_k}^{\theta_k + \Delta\theta_k} e^{-jx \sin y} dy$. From [9], the power spectrum of $J_0(2\pi f_d m T_s)$ is the well-known "U-shape" function, namely, $S_{J_0}(f) = \frac{1}{\pi f_d \sqrt{1-f^2/f_d^2}}$, $f \in [-f_d, f_d]$. Therefore, the bandwidth of (8) is upper bounded by f_d . Moreover, it also shows that no matter what the range of the spatial AS is, it will not affect this time-domain bandwidth of $h_{k,q}(n)$.

Since that $\tilde{h}_{k,q}(n) = \sum_{i=0}^{M-1} h_{k,i}(n) e^{-j\frac{2\pi}{M}iq}$, we then have

$$\begin{aligned} &\mathbb{E}\{\tilde{h}_{k,q}(n)\tilde{h}_{k,q}^*(n+m)\} \\ &= \sum_{i=0}^{M-1} \sum_{l=0}^{M-1} \mathbb{E}\{h_{k,i}(n)h_{k,l}^*(n+m)\} e^{-j\frac{2\pi}{M}q(i-l)}. \end{aligned} \quad (9)$$

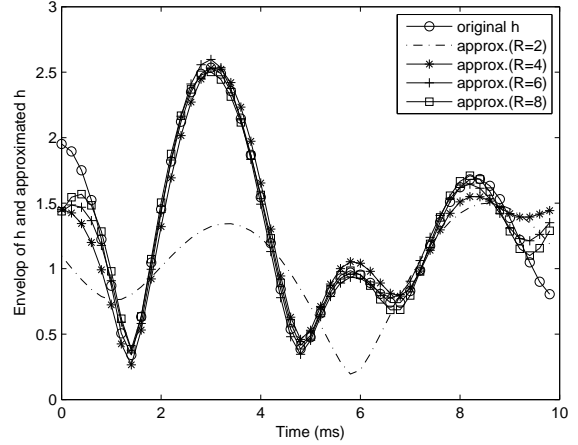


Fig. 3. CE-BEM approximation of $\tilde{h}_{k,2}(n)$, $n = 1, \dots, N$ with different values of R , where $M = 128$, $d = \lambda/2$, $f_d = 200\text{Hz}$, $T_s = 0.1\text{ms}$ and $N = 100$.

This correlation function is the superimposition of multiple band-limited signals and thus the property is obvious. ■

Following *Property 2*, the CE-BEM approximation of band-limited signals in (4) is then justified and the order R should be at least $2\lceil f_d N T_s \rceil$ in order to provide sufficient degrees of freedom [7]. To illustrate this, an approximation example of $\tilde{h}_{k,2}(n)$ is given in Fig. 3, where the simulation parameters are taken as $M = 128$, $d = \lambda/2$, $f_d = 200\text{Hz}$, $T_s = 0.1\text{ms}$ and $N = 100$. It can be seen that when $R \geq 2\lceil f_d N T_s \rceil = 4$, the CE-BEM approximation of $\tilde{h}_{k,2}(n)$ is pretty good. However, for $R = 2$ the ambiguous estimation appears due to the lack of sufficient sampling degrees of freedom.

Combining above two properties, the approximation of massive MIMO time-varying channels can be simplified as

$$\begin{aligned} \mathbf{h}_k(n) &\approx \sum_{q \in \mathcal{B}_k} \tilde{h}_{k,q}(n) \mathbf{f}_q = \sum_{q \in \mathcal{B}_k} \sum_{r=0}^R \lambda_{k,q}^r e^{j2\pi(r-R/2)n/N} \mathbf{f}_q \\ &= \sum_{q \in \mathcal{B}_k} \boldsymbol{\lambda}_{k,q}^T \mathbf{c}_n \mathbf{f}_q, \quad n = 0, \dots, N-1, \end{aligned} \quad (10)$$

where $\boldsymbol{\lambda}_{k,q} = [\lambda_{k,q}^0, \dots, \lambda_{k,q}^R]^T$ and $\mathbf{c}_n = [e^{-j\frac{2\pi n}{N}\frac{R}{2}}, \dots, e^{j\frac{2\pi n}{N}\frac{R}{2}}]^T$. Generally, (10) can be viewed as a joint *spatial-temporal BEM* (ST-BEM) for massive MIMO fast-fading channels.

III. CHANNEL ESTIMATION SCHEME WITH ST-BEM

In this section, we consider the uplink/downlink transmission that utilizes the spatial signatures to realize the orthogonal training among different users with much reduced overhead. The transmissions between BS and users always start from an uplink preamble to obtain the spatial signature of each user. Then users are grouped for uplink/downlink training based on their spatial signatures.

The pilot symbol aided modulation (PSAM) technique [11] is employed to probe the uplink/downlink time-varying channels, where pilot symbols are inserted among information symbols in each interval of NT_s . Let us define $\mathcal{T}_t =$

$\{n_0, n_1, \dots, n_{T-1}\} \subset \{0, \dots, N-1\}$ as the time index set for pilot symbols.

A. Obtain Spatial Information through Uplink Preamble

Since the AS information for all users will keep unchanged for a relative long time, then users can be scheduled during the preamble period to yield the initial channel estimate $\hat{\mathbf{h}}_k^{\text{pre}}$ for $k = 1, \dots, K$, respectively, by using existing conventional uplink channel estimation methods, e.g. least square (LS) and minimum mean square error (MMSE). And the next step is to extract the spatial signature \mathcal{B}_k of size τ that contains the maximum power of $\mathbf{F}\mathbf{h}_k^{\text{pre}}$ for each user.

B. Uplink Training with User Grouping

Keep in mind that the non-overlapped properties of different users' spatial signatures could be utilized to release the pressure of training overheads. Let us divide users into separate groups according to their spatial signatures. Specifically, users are allocated to the same group if their spatial signatures do not overlap, i.e., $\mathcal{B}_k \cap \mathcal{B}_l = \emptyset$. Assume that all users are divided into G groups and denote the user index set of the g -th group as \mathcal{U}_g . We expect that $G \ll K$ since the cardinality of \mathcal{B}_k , namely, the number of selected components of channels, is set as $\tau = |\mathcal{B}_k|$ which is much smaller than M . Meanwhile, users are randomly distributed in the service region such that their spatial signatures will also be randomly distributed.

As channels of different users in the same group could be discriminated by their spatial signatures, we could assign the same pilot sequence to all users in one group. Then let us specify the received training signals at BS as $\mathbf{Y} = [\mathbf{y}(n_0), \mathbf{y}(n_1), \dots, \mathbf{y}(n_{T-1})] \in \mathbb{C}^{M \times T}$ and the common transmitted pilot symbols of users in g -th group as $\mathbf{S}_g = \text{diag}\{s_g(n_0), s_g(n_1), \dots, s_g(n_{T-1})\}$ with $\sum_{i=0}^{T-1} |s_g(n_i)|^2 = 1$. Then we have

$$\begin{aligned} \mathbf{Y} &= \sum_{g=1}^G \sum_{k \in \mathcal{U}_g} [\mathbf{h}_k(n_0), \dots, \mathbf{h}_k(n_{T-1})] \sqrt{P_k^{\text{ul}}} \mathbf{S}_g + \mathbf{N} \\ &= \sum_{g=1}^G \sum_{k \in \mathcal{U}_g} \sqrt{P_k^{\text{ul}}} \mathbf{F}^H \mathbf{\Lambda}_k \mathbf{C} \mathbf{S}_g + \mathbf{N} \\ &= \mathbf{F}^H \left[\sum_{k \in \mathcal{U}_1} \sqrt{P_k^{\text{ul}}} \mathbf{\Lambda}_k, \dots, \sum_{k \in \mathcal{U}_G} \sqrt{P_k^{\text{ul}}} \mathbf{\Lambda}_k \right] \\ &\quad \cdot [(\mathbf{C} \mathbf{S}_1)^H, \dots, (\mathbf{C} \mathbf{S}_G)^H]^H + \mathbf{N} \\ &= \mathbf{F}^H \mathbf{\Lambda} [(\mathbf{C} \mathbf{S}_1)^H, \dots, (\mathbf{C} \mathbf{S}_G)^H]^H + \mathbf{N} \end{aligned} \quad (11)$$

where P_k^{ul} is the uplink power constraint at user- k ; $\mathbf{\Lambda}_k = [\lambda_{k,0}, \lambda_{k,1}, \dots, \lambda_{k,M-1}]^T$ denotes the CE-BEM coefficients for user- k ; $\mathbf{C} = [\mathbf{c}_{n_0}, \mathbf{c}_{n_1}, \dots, \mathbf{c}_{n_{T-1}}]$ and \mathbf{N} is the noise matrix whose elements are i.i.d. $\mathcal{CN}(0, \sigma_n^2)$.

When $T \geq G(R+1)$, there will be adequate observations to estimate all the unknowns in $\mathbf{\Lambda}$. In this paper, we resort to the LS estimator as [7] did and then obtain

$$\hat{\mathbf{\Lambda}} = \mathbf{F} \mathbf{Y} \left\{ [(\mathbf{C} \mathbf{S}_1)^H, \dots, (\mathbf{C} \mathbf{S}_G)^H]^H \right\}^\dagger, \quad (12)$$

and the mean square error (MSE) is given as

$$\mathbb{E}\{\|\hat{\mathbf{\Lambda}} - \mathbf{\Lambda}\|_F^2\} = M \sigma_n^2 \text{tr} \left\{ \left([(\mathbf{C} \mathbf{S}_1)^H, \dots, (\mathbf{C} \mathbf{S}_K)^H]^H \cdot [(\mathbf{C} \mathbf{S}_1), \dots, (\mathbf{C} \mathbf{S}_K)] \right)^{-1} \right\} \quad (13)$$

In line with the idea of [7], we know that to minimize the MSE in (13), the optimal pilot symbols adopted by users should satisfy the following constraints as

$$\mathbf{C} \mathbf{S}_g \mathbf{S}_g^H \mathbf{C}^H = \mathbf{I}_{R+1}, \quad \mathbf{C} \mathbf{S}_g \mathbf{S}_{g'}^H \mathbf{C}^H = \mathbf{0}_{R+1}, \quad \forall g \neq g'. \quad (14)$$

Moreover, the optimal pilot symbols for different groups are proved to be equi-powered, equi-spaced over $\{0, \dots, N-1\}$, and phase shift orthogonal. One example of such kind of pilot sequences is

$$s_g(n_i) = \sqrt{1/T} e^{j2\pi i(g-1)(R+1)/T}, \quad g = 1, \dots, G; i = 0, \dots, T-1. \quad (15)$$

Let us then focus on user- k in group- g and get

$$\hat{\mathbf{\Lambda}}_k = \mathbf{\Lambda}_k + \sum_{l \in \{\mathcal{U}_g \setminus k\}} \sqrt{P_l^{\text{ul}}/P_k^{\text{ul}}} \mathbf{\Lambda}_l + \frac{1}{\sqrt{P_k^{\text{ul}}/\sigma_n^2}} \mathbf{N}_k, \quad (16)$$

where $\mathbf{N}_k \in \mathbb{C}^{M \times R+1}$ has the i.i.d. $\mathcal{CN}(0, 1)$ elements. Considering the disjoint spatial signatures of users in the same group, we can straightforwardly extract

$$\begin{aligned} [\hat{\mathbf{\Lambda}}_k]_{\mathcal{B}_k, :} &= [\hat{\mathbf{\Lambda}}_k]_{\mathcal{B}_k, :} = [\mathbf{\Lambda}_k]_{\mathcal{B}_k, :} + \sum_{l \in \{\mathcal{U}_g \setminus k\}} \sqrt{P_l^{\text{ul}}/P_k^{\text{ul}}} [\mathbf{\Lambda}_l]_{\mathcal{B}_k, :} \\ &\quad + 1/\sqrt{P_k^{\text{ul}}/\sigma_n^2} [\mathbf{N}_k]_{\mathcal{B}_k, :}, \quad \forall k \in \mathcal{U}_g. \end{aligned} \quad (17)$$

Bearing in mind that \mathcal{B}_l and \mathcal{B}_k are kept away from each other, we know the entries of $[\mathbf{\Lambda}_l]_{\mathcal{B}_k, :}$ in (17) are negligible such that the pilot contamination term caused by reusing the same pilot in one group is immediately reduced, and then $\mathbf{\Lambda}_k$ for user- k can be approximated as

$$\mathbf{\Lambda}_k = \begin{bmatrix} \mathbf{0}^T & [\hat{\mathbf{\Lambda}}_k]_{\mathcal{B}_k, :}^H & \mathbf{0}^T \end{bmatrix}^H, \quad (18)$$

where the two all-zero matrices $\mathbf{0}$ have appropriate sizes. With this estimated coefficients in hand, the channel estimate $\hat{\mathbf{h}}_k(n)$ thus can be obtained by (10).

Remark 1: By grouping users according to their spatial signatures, the total pilot overheads can be reduced significantly from $T = K(R+1)$ to $T = G(R+1)$ with $G \ll K$. Furthermore, the operations in (6) and (10) can be accelerated by partial fast Fourier transform (FFT) [10], which further moderates the high calculation complexity.

C. Downlink Channel Representation with Angle Reciprocity

Denote the downlink channel from BS to user- k as $\mathbf{g}_k^H(n) \in \mathbb{C}^{1 \times M}$. Similar to (10), $\mathbf{g}_k(n) \in \mathbb{C}^{M \times 1}$ can be modeled as

$$\mathbf{g}_k(n) \approx \sum_{q \in \mathcal{B}'_k} \tilde{g}_{k,q}(n) \mathbf{f}_q = \sum_{q \in \mathcal{B}'_k} \lambda_{k,q}^{d^T} \mathbf{c}_n \mathbf{f}_q, \quad (19)$$

where $\lambda_{k,q}^d$ denotes the CE-BEM coefficients of downlink channels and \mathcal{B}'_k is the downlink version of spatial signatures.

All other parameters have been defined in (11). Similar to the uplink, once \mathcal{B}'_k is determined, the downlink channel estimation for $\mathbf{g}_k(n)$ will be simplified to estimating those remaining unknown coefficients $\lambda_{k,q}^d$'s.

To determine \mathcal{B}'_k , let us first introduce an important property of wireless channels. Since the propagation path of electromagnetic wave is reciprocal, we know that only the signal wave that physically reverses the uplink path can reach the user during the downlink period. Hence, downlink signals that could effectively arrive at the user should have the same DOD spread as the uplink DOA spread. We call this property as the *angle reciprocity*. Similar assumptions have already been directly adopted in many existing works, such as [12], [13].

Based on the angle reciprocity and bearing in mind that the spatial signatures are exactly determined by the AS, we know that \mathcal{B}'_k can be directly determined by \mathcal{B}_k . Specifically, according to *Property 1*, we will have

$$\sin \theta_k = \frac{q\lambda_1}{Md} = \frac{q'\lambda_2}{Md}, \text{ with } q \in \mathcal{B}_k, q' \in \mathcal{B}'_k, \quad (20)$$

where λ_1 and λ_2 denote the uplink/downlink carrier wavelengths, respectively. Then the integer set \mathcal{B}'_k can be expressed as $\mathcal{B}'_k = \{q'_{\min}, q'_{\min} + 1, \dots, q'_{\max}\}$ with

$$q'_{\min} = \left\lfloor \frac{\lambda_1}{\lambda_2} q_{\min} \right\rfloor, \quad q'_{\max} = \left\lceil \frac{\lambda_1}{\lambda_2} q_{\max} \right\rceil, \quad (21)$$

where $q_{\min} \leq q \leq q_{\max}, \forall q \in \mathcal{B}_k$.

D. Downlink Training with User Grouping

Following (19), the effective dimensions of downlink channels for all users have been reduced to $\tau \ll M$, and thus by adopting the uplink user grouping strategy directly, users in each groups can be simultaneously scheduled for downlink transmission with only $T = \tau(R + 1)$ pilot symbols required.

Similar to the uplink training procedures, we have the received $\mathbf{y}_k^d = [y_k(n_0), \dots, y_k(n_{T-1})]^T$ at user- k in \mathcal{U}_g as

$$\begin{aligned} \mathbf{y}_k^d &= \sum_{l \in \mathcal{U}_g} \sum_{1 \leq i \leq \tau, q_i \in \mathcal{B}_i} \sqrt{P_l^{\text{dl}}/\tau} \mathbf{S}_i^d \mathbf{C}^T \lambda_{k,q_i}^d + \mathbf{n}_k \\ &= \sum_{l \in \mathcal{U}_g} [\mathbf{S}_1^d \mathbf{C}^T, \dots, \mathbf{S}_\tau^d \mathbf{C}^T] \text{vec} \left([\mathbf{\Lambda}_k^d]_{\mathcal{B}_k, \cdot}^T \right) + \mathbf{n}_k, \end{aligned} \quad (22)$$

where diagonal matrices $\mathbf{S}_i^d \in \mathbb{C}^{T \times T}, i = 1, \dots, \tau$ denote the transmitted pilot sequence for all users in \mathcal{U}_g at their own τ beam directions \mathbf{f}_q 's respectively, and P_l^{dl} is the total downlink power constraint for user- l . Moreover, $\mathbf{\Lambda}_k^d$ is the downlink version of $\mathbf{\Lambda}_k$ and noise vector satisfies $\mathbf{n}_k \sim \mathcal{CN}(\mathbf{0}, \sigma_n^2 \mathbf{I}_T)$.

Like (15), the optimal pilot sequences $\mathbf{S}_i^d \in \mathbb{C}^{T \times T}, i = 1, \dots, \tau$ for (22) are also equi-powered, equi-spaced and phase shift orthogonal. Then the downlink channels can be recovered similarly, procedures of which are omitted due to space limitations. To complete the channel estimation, each user only has to feed back τ components $[\mathbf{\Lambda}_k^d]_{\mathcal{B}_k, \cdot}$ to BS.

Remark 2: It can be found that user- k does not need the knowledge of spatial signature set \mathcal{B}_k to perform the estimation of $[\mathbf{\Lambda}_k^d]_{\mathcal{B}_k, \cdot}$. This removes the necessity of feedback from BS

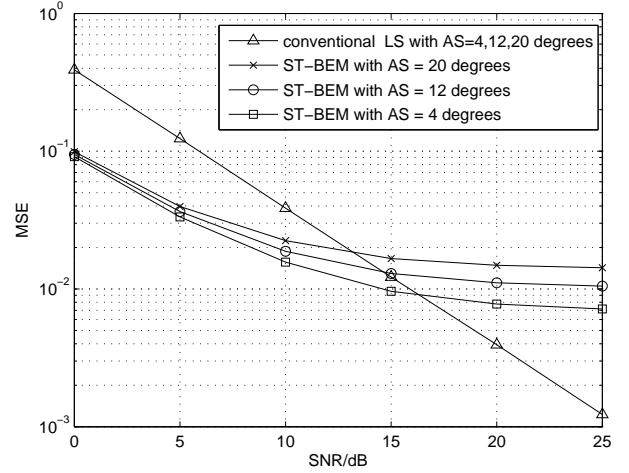


Fig. 4. Uplink MSE performance comparison of ST-BEM with $T=G(R+1)=15$ and conventional LS with $T=K(R+1)=60$. Two-side AS is set as $4^\circ, 12^\circ, 20^\circ$, respectively.

to the user and is thus a key advantage that makes the proposed downlink channel estimation strategy suitable for fast-fading environments.

IV. SIMULATIONS

In this section, we demonstrate the effectiveness of the proposed strategy through numerical examples. We select $M=128, d=\lambda/2$ and consider $K=12$ users gathered into 4 disjoint clusters in the coverage area. Channel vectors are formulated according to (1), where $P=100, f_d=200$ Hz, $T_s=1$ us; θ_{kp} is uniformly distributed inside $[\theta_k - \Delta\theta_k, \theta_k + \Delta\theta_k]$, where two-side AS is supposed be $2\Delta\theta_k=4^\circ, 12^\circ, 20^\circ$, respectively. The value of τ is assumed to be $\tau=16$, which is only $1/8$ of the antenna number. Moreover, we select $R=4, N=K(R+1)=60$ for uplink and $N=M(R+1)=640$ for downlink, which satisfies the requirement of $R \geq 2\lceil f_d N T_s \rceil$. The performance metric of channel estimation is the normalized MSE, i.e.,

$$\text{MSE} \triangleq \frac{\sum_{k=1}^K \sum_{n=0}^{N-1} \|\mathbf{h}_k(n) - \hat{\mathbf{h}}_k(n)\|^2}{\sum_{k=1}^K \sum_{n=0}^{N-1} \|\mathbf{h}_k(n)\|^2}.$$

Fig. 4 compares the proposed ST-BEM with the conventional LS method for uplink MSE. To apply the conventional LS, all $N=K(R+1)=60$ symbols are necessary for uplink training, while only $T=G(K+1)=15$ out of total $N=60$ symbols are enough for ST-BEM. To provide a fair comparison, for any given SNR ρ , the uplink training power for each user is kept the same $P_k^{\text{ul}}=T\rho$ for both methods. Moreover, different values of AS are also considered. It can be seen that as the SNR increases, there are error floors for ST-BEM curves and the error floor is higher with larger AS. This phenomenon is not unexpected due to the truncation error of SBEM from the real channel and can also be observed in CE-BEM [3]. It is seen that when the sufficient length of training is available and when the computational complexity is acceptable, then the conventional LS method does not have the error floor for any

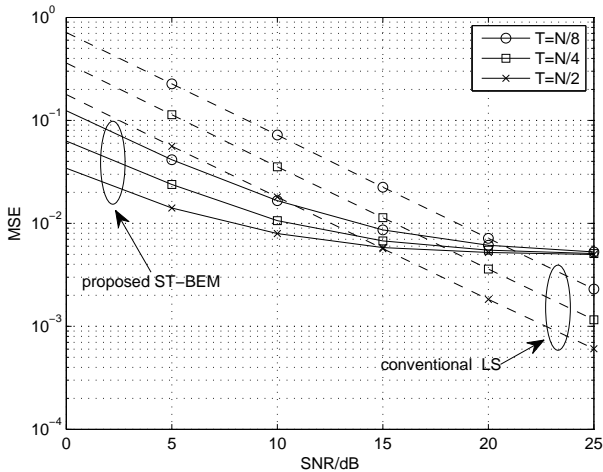


Fig. 5. Downlink MSE performance comparison of ST-BEM with $T = N/8, N/4, N/2$, respectively, and conventional LS with $T = M(R + 1) = N$. Two-side AS is set as 4° .

AS values. Nevertheless, it can be observed that the channel estimation from ST-BEM outperforms the conventional method when SNR is relatively low (≤ 15 dB). The reasons can be found from (17) where the proposed method only involves τ components of the noise vector while the conventional LS method includes the whole noise power.

Fig. 5 compares the downlink MSE performances of ST-BEM with $T=N/8, N/4, N/2$, and conventional LS with all $N = M(R + 1)$ symbols. The total power constraint are kept the same $\sum_{k=1}^K P_k^{\text{dl}} = KT\rho$ for both methods to ensure the fairness. It can also be found that the proposed ST-BEM is superior to conventional LS, not only for the higher estimation accuracy in relative low SNR regions, but also due to the less training overheads, which will help to increase the system spectral efficiency.

Lastly, we show the bit error rate (BER) performance under QPSK modulation for the downlink data transmission in Fig. 6. Three kinds of CSI are compared, i.e., perfect CSI, CSI from the proposed ST-BEM, and CSI from the conventional LS. To keep the comparison fair, the overall training and data transmission power are set as the same for each method. It is seen that the BER achieved by ST-BEM is better than that of conventional LS and has about 0.5 dB gap from that of perfect CSI, which corroborates the effectiveness of the proposed ST-BEM.

V. CONCLUSIONS

In this paper, we investigated the uplink/downlink training for multiuser massive MIMO systems in time-varying environments. We exploited the characteristics of ULA and proposed a simple DFT-based ST-BEM to represent channel vectors with reduced parameter dimensions in both spatial and time domains, which helps to reduce the training and feedback overhead significantly. Meanwhile, the uplink spatial signatures could also be used to simplify the downlink training based on the angle reciprocity, making the proposed ST-BEM

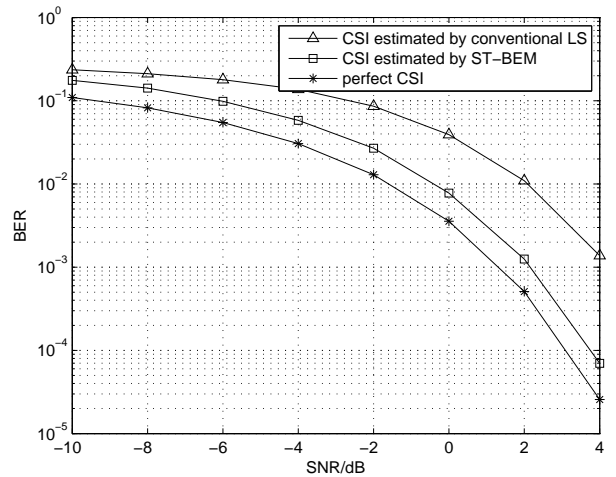


Fig. 6. The downlink BER performance comparison of the proposed ST-BEM method with $T = N/8$ and the conventional LS method with $T = N$. Two-side AS is set as 4° .

applicable for both TDD and FDD massive MIMO time-varying systems. Numerical results have demonstrated the effectiveness of the proposed scheme.

REFERENCES

- [1] T. L. Marzetta, "Noncooperative cellular wireless with unlimited numbers of base station antennas," *IEEE Trans. Wireless Commun.*, vol. 9, no. 11, pp. 3590–3600, Nov. 2010.
- [2] G. Arredondo, W. H. Chriss, and E. H. Walker, "A multipath fading simulator for mobile radio," *IEEE Trans. Commun.*, vol. 21, no. 11, pp. 1325–1328, Jan. 2003.
- [3] G. B. Giannakis and C. Tepedelenlioglu, "Basis expansion models and diversity techniques for blind identification and equalization of time-varying channels," *Proc. IEEE*, vol. 86, no. 10, pp. 1969–1986, Oct. 1998.
- [4] A. Adhikary, J. Nam, J. Y. Ahn, and G. Caire, "Joint spatial division and multiplexing—the large-scale array regime," *IEEE Trans. Inf. Theory*, vol. 59, no. 10, pp. 6441–6463, Oct. 2013.
- [5] H. Yin, D. Gesbert, M. Filippou, and Y. Liu, "A coordinated approach to channel estimation in large-scale multiple-antenna systems," *IEEE J. Sel. Areas Commun.*, vol. 31, no. 2, pp. 264–273, Feb. 2013.
- [6] Y. R. Zheng and C. Xiao, "Simulation models with correct statistical properties for rayleigh fading channels," *IEEE Trans. Commun.*, vol. 51, no. 6, pp. 920–928, June 2003.
- [7] G. Wang, F. Gao, W. Chen, and C. Tellambura, "Channel estimation and training design for two-way relay networks in time-selective fading environments," *IEEE Trans. Wireless Commun.*, vol. 10, no. 8, pp. 2687–2691, August 2011.
- [8] C. W. R. Chiong, Y. Rong, and Y. Xiang, "Channel estimation for time-varying MIMO relay systems," *IEEE Trans. Wireless Commun.*, vol. 14, no. 12, pp. 6752–6762, Dec. 2015.
- [9] R. H. Clarke, "A statistical theory of mobile-radio reception," *Bell System Technical Journal*, vol. 47, no. 6, pp. 957–1000, July 1968.
- [10] S. He and M. Torkelson, "Computing partial DFT for comb spectrum evaluation," *IEEE Signal Process. Lett.*, vol. 3, no. 6, pp. 173–175, June 1996.
- [11] J. K. Cavers, "An analysis of pilot symbol assisted modulation for Rayleigh fading channels," *IEEE Trans. Veh. Technol.*, vol. 40, no. 4, pp. 686–693, Nov. 1991.
- [12] A. Kuchar, M. I. Tangemann, and E. Bonek, "A real-time DOA-based smart antenna processor," *IEEE Trans. Veh. Technol.*, vol. 51, no. 6, pp. 1279–1293, Nov. 2002.
- [13] K. Hugl, K. Kalliola and J. Laurila, "Spatial reciprocity of uplink and downlink radio channels in FDD systems," in *COST 273 TD(02)066*, 2002.